Analyst

ROYAL SOCIETY OF CHEMISTRY

PAPER

View Article Online
View Journal

Cite this: DOI: 10.1039/d1an00313e

A polyA DNA probe-based ultra-sensitive and structure-distinguishable electrochemical biosensor for the analysis of RNAi transgenic maize†

Li Xu,‡[a] Jiawei Qi,‡[a,b] Yanli Wen,[a] Wen Liang,[a] Lele Wang,[a] Zhenzhou Yang,[a] Xue Yang,[a] Yu Qi,[a] Manlei Duan,[a] Keke Zhao,[a] Jie Gu,[a] Yiji Shen,[a] Pinhua Rao,[b] Min Ding,[a] Shuzhen Ren,[a] Liang Li*[c] and Gang Liu *[a]

Received 20th February 2021,
Accepted 26th March 2021

DOI: 10.1039/d1an00313e

rsc.li/analyst

Since the application of RNA interference (RNAi) is rapidly developing in GMO technology, accurate and sensitive detection of functional RNA molecules was urgently needed, for the safety and functional assessment of RNAi crops. In this work, we developed an electrochemical biosensor for transgene-derived long RNA based on a poly-adenine (polyA) DNA capture probe. The polyA self-assembling monolayer (SAM) provided enhanced interface stability and optimized surface density for the subsequent hybridization of the long RNA molecule. A multiple reporter probe system (MRP) containing 12 reporter probes (RPs) and 2 spacers was applied to open the complex molecular secondary structure and hybridize with the long RNA, with the critical assistance of dimethyl sulfoxide (DMSO). By using 3 addressable RPs, structural recognition was performed among long stem-loop RNA, long dsRNA (no loop), and siRNA. Excellent selectivity was achieved when the extracted total RNA samples were directly analyzed. When reverse transcription recombinase polymerase amplification (RT-RPA) technology was combined, the sensitivity was improved to 10 aM. To the best of our knowledge, this is the first electrochemical biosensor with the excellent capability of quantification and structural analysis of the long RNA of the RNAi GMO. Our work shows great potential in a wide range of RNAi GMO samples.

Introduction

The RNA interference (RNAi) process was firstly found in eukaryotic organisms, regulating gene expression mediated by double-stranded RNA (dsRNA) with homology to a target gene.[1–3] Recently, RNAi technology has been applied in agricultural biotechnology to control a variety of target organisms, such as insects,[4–6] bacteria,[7] fungi,[8] viruses,[9,10] and even parasitic plants.[11] RNAi transgenic approaches offer many advantages over the traditional and hazardous chemical methods of pest control.[12] They are more economical, efficient, stable, flexible, and environment/farmer-friendly. However, potential risks associated with RNAi technology should be considered, such as unintended gene silencing, potential toxicity to humans and the environment, *etc*.[13–15] On the other hand, the functional characterization of RNAi genetically modified organisms (GMOs) is also important for quality control. Since RNAi GMOs do not express any novel kinds of protein other than RNA, RNA detection is the only way for RNAi analysis. Unfortunately, challenges remain to accurately and sensitively detect RNA with complex secondary structures in plant samples.[16]

The reverse transcription polymerase chain reaction (RT-PCR) is the main method for RNAi GMO analysis[17] with excellent sensitivity, but its specificity may be limited if inverted RNA repeats or self-priming of RNA occurs. Furthermore, the complex operation and cumbersome instruments of the RT-PCR hindered its application for on-site analysis. More importantly, we usually need to perform sample purification to eliminate genomic DNA containing cognate sequences before RT-PCR. Thus, the development of new strategies for the specific detection of RNA molecules in RNAi GMOs or environmental samples to support the safety and functional assessment is urgently needed.[17,18] Scientists in

[a]*Laboratory of Biometrology, Division of Chemistry and Ionizing Radiation Measurement Technology, Shanghai Institute of Measurement and testing technology, Shanghai, 201203, P.R. China. E-mail: liug@simt.com.cn*
[b]*College of Chemistry and Chemical Engineering, Shanghai University of Engineering Science, Shanghai, 201620, P.R. China*
[c]*Biotechnology Research Institute, Chinese Academy of Agricultural Sciences, Beijing 100081, China*

†Electronic supplementary information (ESI) available. See DOI: 10.1039/d1an00313e

‡These authors contributed equally.

Monsanto Company[18] developed a detection strategy based on the QuantiGene assay platform (Affymetrix, Inc.). They successfully detected 10 pg of dsRNA per g of fresh tissue, and the reproducibility was well demonstrated. However, their hybridization needs a very long time (overnight), and thus it is very important to develop faster and portable RNAi analysis methods, and novel biosensors with advanced sensitivity and high-speed are needed.

Electrochemical nucleic acid biosensors (E-biosensors) have shown great advantages such as low cost, time-saving, portability, easy-operation, and high sensitivity in DNA target detection.[19–26] However, the application of E-biosensors in RNAi GMO analysis is still facing several challenges: firstly, the combination of biosensor probes is usually very difficult because the targets are inverted, containing RNA transcripts with very complex secondary structures. Secondly, the length of the RNA is usually up to 1000 nt, which exceeds the classic working range of the traditional E-biosensors. Thirdly, improved selectivity is needed when facing complex plant matrices.

To overcome these challenges, we developed a poly-adenine (PolyA) probe-based E-biosensor for RNA detection in RNAi-based transgenic maize, employing the high affinity between polyA-tail and the gold surface.[24,25] We designed a multiple reporter probe (MRP) system containing 12 RPs and 2 spacers, which combined with the RNA in a staggered distribution along the RNA molecule. MRPs in our work not only brought increased reporter labels but also provided critical assistance during the unfolding of the RNA. The base-stacking force of the multi-probe on the target RNA plays a more important role than the hydrogen bonds. On the other hand, we applied dimethyl sulfoxide (DMSO) to weaken the intramolecular hybridization and facilitate the combination of the MRP. Critical experimental conditions were systematically optimized, including the length of the polyA tail and the hybridization of the MRP. By using addressable RPs, we performed the structural analysis on the electrochemical interface.

Experimental section

Materials

RNAi-mediated transgenic maize events (DBN11061, DBN11048, and DBN11019) in this study were provided by Beijing Dabeinong Biotechnology Co., Ltd (Beijing, China). The leaf tissues of transgenic maize were collected at the V3–V4 stage. Samples were frozen on dry ice before being stored at −80 °C. An 852 bp DNA fragment of RNA was synthesized and cloned by Bioligo (Shanghai, China). All oligonucleotides were synthesized by Bioligo (Shanghai, China). The DNA sequences used in this study are listed in Table 1. MCH, DMSO, and diethyl pyrocarbonate (DEPC) were purchased from Sigma-Aldrich (St Louis, MO). The HRP substrate TMB (TMB = 3,3′,5,5′ tetramethylbenzidine) was purchased from Neogen (USA) in the form of a ready-to-use reagent (Enhanced K-Blue TMB Substrate, H_2O_2 included). Avidin horseradish peroxidase (avidin-HRP) was purchased from eBioscience (San Diego, CA). The diluent buffer was purchased from Fitzgerald Industries International (Acton, MA). The plant total RNA extraction kit, RNA purification kit, and *in vitro* transcription kit were purchased from Thermo Fisher (USA). The Ex Taq enzyme, DNA fragment purification kit, and 1st strand cDNA synthesis kit were purchased from Takara (Dalian, China). The plasmid extraction kit was purchased from Macherey-Nagel (USA). The bioanalyzer RNA analysis kit was purchased from Agilent (USA). The RPA kit (TwistAmp™ Liquid Basic) containing reagents for RNA amplification was obtained from TwishtDx Ltd (Cambridge, UK). All other chemicals were at least of analytical grade. All solutions were prepared using DEPC-treated Milli-Q water (18 MΩ cm resistivity) from a Millipore system.2.2 Design of oligonucleotide probes.

Table 1 DNA sequences' information

Name	Sequence (5′–3′)
CP-A30-1	A30TTGTCTTGTGCTGCTGGCGCGCCC-TAGTGGCCGCT
CP-A30-2	A30TTGTCTTGTGCTGCTGGCGCGCCCTAG-TGGCCGCTTGGTA
CP-A20	A20TTGTCTTGTGCTGCTGGCGCGCCCTAGT-GGCCGCTTGGTA
CP-A40	A40TTGTCTTGTGCTGCTGGCGCGCCCTAGTG-GCCGCTTGGTA
RP-5	GCTCTTCCTAAAGCCAACAA-biotin
RP-5-RC	TTGTTGGCTTTAGGAAGAGC
RP-6	AACAACTTGTTTATGAATA-biotin
Spacer-1	CAGTAGCGGAAGCATTTCT
Spacer-2	GATCGCAGTACTTCTTTTTA
RP-7	AGTTCTAGGTCCTTGTTCAA-biotin
RP-8	TGAATTTGTTTCAGTCTTGC-biotin
RP-9	CGTCAACCTGTAATTGTTTC-biotin
RP-10	CAAGTGCACTGGAACTCCAT-biotin
RP-11	TTATCTTTAACTCCACCTTT-biotin
RP-16	TCACATCACAGCGTTAACGC

The reporter probe (RP) was complementary to the target sequence and had a biotin label at the 5′ end. The capture probes (CPs) consisted of 2 parts: a capturing fragment that was complementary to the target RNA and an assembling part containing 30 consecutive adenines (PolyA). All the gene sequences are listed in Table 1.

In vitro transcription of the long stem-loop RNA

An 852 bp DNA fragment containing 261 bp inverted repeats and 98 bp neutral spacer of RNA was synthesized and cloned into pET-28a (+) vector with a T7 promoter. Then a 1034 bp fragment containing the target RNA and a T7 promoter was amplified by PCR from the recombinant plasmid. The PCR product was purified using a gel purification kit and used as the template DNA for *in vitro* transcription. For *in vitro* RNA synthesis, the purified PCR product was incubated with RNA polymerase in transcription buffer for 1 h at 37 °C. The transcription reaction mixture was then treated with DNase I at 37 °C for 30 minutes to remove the template DNA and then cleaned using an RNA purification kit. The produced RNA was used as the reference standard for the development of an

E-biosensor. The size and purity was confirmed using a bioanalyzer (Agilent 2100), and its concentration was measured using a UV and visible spectrometer (Nanodrop-2000, Thermo Fisher, USA). Aliquots of the RNA sample were kept at −80 °C.

Plant RNA extraction

For the extraction of plant total RNA, frozen maize leaf tissues were ground to a fine powder in a mortar chilled with liquid nitrogen. Then the powder was transferred to the lysis buffer and purified using a plant total RNA extraction kit. The purity and integrity were evaluated using a bioanalyzer and the concentration was determined to be 3635.5 ng μL^{-1}, using a UV-visible spectrum (Nanodrop-2000). The purified total RNA was stored at −80 °C for long-term storage.

Construction of the polyA-based biosensing surface

The gold working electrode was from CH Instruments Inc (2 mm-diameter). Gold electrodes were cleaned following a reported protocol.[27] Detailed information about electrode treatment is provided in the ESI (section 4).† The cleaned electrodes were then incubated in assembling buffer (pH 7.4, 10 mM Tris·HCl, 1 M NaCl, 1 mM EDTA) containing a 1 μM polyA-based capture probe overnight at 45 °C. Then, the modified electrodes were treated with 100 μL of MCH solution (0.1 mM) for 1 h at room temperature (RT). After the MCH passivation, the gold electrode was rinsed thoroughly with the washing buffer (0.01 M PBS containing 10 mM PB buffer and 0.01 M NaCl), and then blow-dried with nitrogen.

Pre-hybridization

Firstly, the target RNA was mixed with the biotinylated RPs and spacers (100 nM) in 10 mM TE buffer (pH 7.4, 10 mM Tris·HCl, 1 mM EDTA) containing 1 M NaCl for 10 min under 95 °C and then cooled down immediately on ice for 20 min.

Electrochemical measurement

The reaction temperature of our E-biosensor was investigated, and finally, 50 °C was found to be the optimum temperature (Fig. S1†). The Pre-hybridization solution (see section "Pre-hybridization") was added onto the capture probe covered electrode and then incubated at 50 °C for 1 h. Then, the gold electrode was rinsed with washing buffer and dried lightly with nitrogen, and then incubated with 3 μL of avidin HRP (500 ng μL^{-1}) for 20 min at RT. Finally, the sensors were rinsed with a washing buffer and subjected to electrochemical measurements in the HRP substrate TMB (Enhanced K-Blue TMB Substrate, H_2O_2 included). Cyclic voltammetry (CV) and amperometric detection were performed using a CHI 630 electrochemical workstation (CH Instruments Inc., Austin), employing a classical three-electrode system following a reported protocol.[28]

In vitro transcription of the target dsRNA without loop

Firstly, two complementary RNA transcripts from DNA templates were synthesized using an Ambion MEGAscript RNAi kit. The RNA strands were hybridized after the transcription reaction to form dsRNA without a loop. Next, DNA templates and any ssRNA were removed with Dnase I and Rnase digestion. Finally, the dsRNA without a loop was purified with a solid-phase adsorption system to remove proteins as well as mono and oligonucleotides.

Preparation of siRNA by endonuclease digestion

The long dsRNA was treated with a dsRNA-specific recombinant bacterial RNase III. The RNaseIII cleaves dsRNA into (12–15) bp dsRNA fragments (siRNA) with 2 to 3 nucleotide 3′ overhangs, and 5′ phosphate and 3′ hydroxyl termini. The termini and overhangs of RNase III cleavage products are thus the same as those produced by Dicer in the eukaryotic RNAi pathway. Then the siRNA products were purified and confirmed using a bioanalyzer (Agilent 2100).

RNA pre-amplification with RT-RPA

A pair of RT-RPA primers was designed for RNA amplification. 50 μL of RT-RPA reaction mix was prepared which contains 1 μL of reverse transcriptase, 1 μL of RNase inhibitor, 0.48 μM primer pairs, 1 μL of RNA sample, and all other solutions provided in the RPA kit following the protocol. The reaction mix was placed on ice for 2 minutes to perform reverse transcription and then incubated at 40 °C for 20 minutes. After that, the amplicons were cleaned and characterized by 3% agarose gel. In this study, a 379 bp DNA fragment from RNA was amplified with RT-RPA and used for further electrochemical detection.

Results and discussion

The strategy of the biosensor

Our RNA analysis was performed on a gold electrode covered by polyA DNA probes, using the strong affinity between polyA and gold surface. The strategy of our E-biosensor is schematically illustrated in Fig. 1A. For the construction and optimization of our biosensor, we take an *in vitro* transcribed RNA (1034 nt) as the target, which folds into a long "stem-loop" RNA structure. To break the secondary structure and perform the hybridization of RPs and CPs, we designed a pre-hybridization process: firstly, the target RNA was mixed with DMSO at high temperature (95 °C), to weaken the intramolecular hydrogen-bonding interaction and improve the accessibility of the RNA target. The pretreated target solution was then cooled down on ice, mixed with 12 biotinylated RPs and 2 spacers immediately. As a result, The RPs and spacers hybridized with the target, forming a zipper-like conformation along the RNA strand.

In the second step of detection, the pre-hybridization solution was added onto the electrode surface covered by the polyA capture probe to form multiple "sandwich-like" structures on the gold electrode surface. It is worth pointing out that the polyA SAM provided high stability and controllable probe density, which is very important for the combination of a large pre-hybridized complex. Finally, avidin-HRP was added to produce an electrochemical catalysis signal that is quantitatively

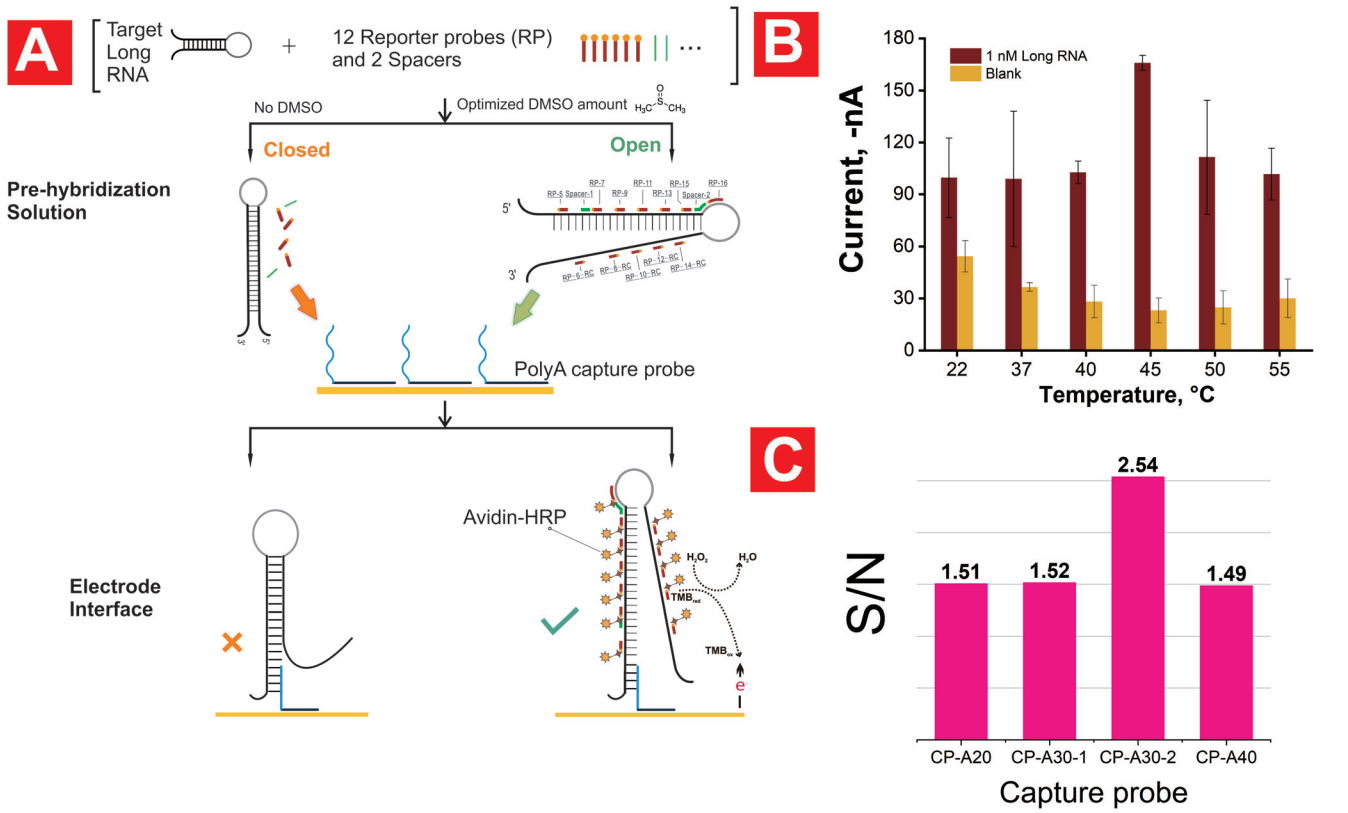

Fig. 1 (A) Schematic illustration of the polyA-based E-biosensor, (B) optimization of the temperature for the self-assembly of the polyA probes (the target was 1 nM long RNA), (C) research about the length of the polyA tail on the capture probes (the target was 10 pM long RNA). (The error bars were based on three repetitive experiments.)

related to the amount of target RNA, in the electrochemical catalysis substrate solution (containing TMB and H_2O_2).

Optimization of the polyA-based biosensor for the analysis of long RNA

As a novel biosensor interface, the polyA-based SAM was systemically researched before being efficiently applied for the analysis of long GMO RNA. Firstly, the assembling temperature was optimized to be 45 °C (Fig. 1B), and then, different capture probes with different lengths of polyA and different capture sequences were applied for the detection of 10 pM target long RNA.

Firstly, it is easy to understand that when using the same length of the polyA section, a longer capture sequence will produce a higher hybridization signal, just as shown in Fig. 1C, CP-A30-2 which had a 4-base longer capture section performed better than CP-A30-1. Then we compared different lengths of the polyA section, with the same capture sequence. Finally, capture probes (CP-A30-2) with 30 adenines achieved the highest signal/noise (S/N) ratio.

It is reported that DMSO can improve the efficiency of DNA hybridization. For example, DMSO was added in PCR amplification,[29–32] to open the secondary structures and hydrogen bonds between base pairs.[33] In this work, we applied DMSO to improve the pre-hybridization of the long RNA, and the concentration of DMSO was optimized according to the concentration level of RNA. 2%–40% (v/v%) DMSO was added into the detection system for the analysis of different levels of target RNA, and the S/N values were compared.

The results showed that (Fig. 2) compared with hybridization reactions without DMSO, the positive signal was significantly increased and the blank signal was reduced when DMSO was added into the reaction mixture. Interestingly, the optimized concentration of DMSO was different according to the concentration of the target RNA. For 200 nM and 10 nM RNA (Fig. 2C and B), 30% DMSO produced the highest S/N ratio. However, for a lower concentration of RNA (1 nM Fig. 2A), the highest S/N ratio occurred at 6% DMSO. A further increase of DMSO suppressed the biosensor signal, probably because excessive DMSO inhibited the hybridization of DNA probes. Accordingly, we used 6% DMSO as the optimized hybridization boosting regent for subsequent experiments.

Design and optimization of the multiple reporter probe (MRP) system

Our electrochemical biosensor used a MRP system to assist the unfolding of the long RNA and amplify the current signal. The experimental results showed that the number and position of the reporter probes on the RNA molecule was very important for the final analytical performance. In general, three MRP

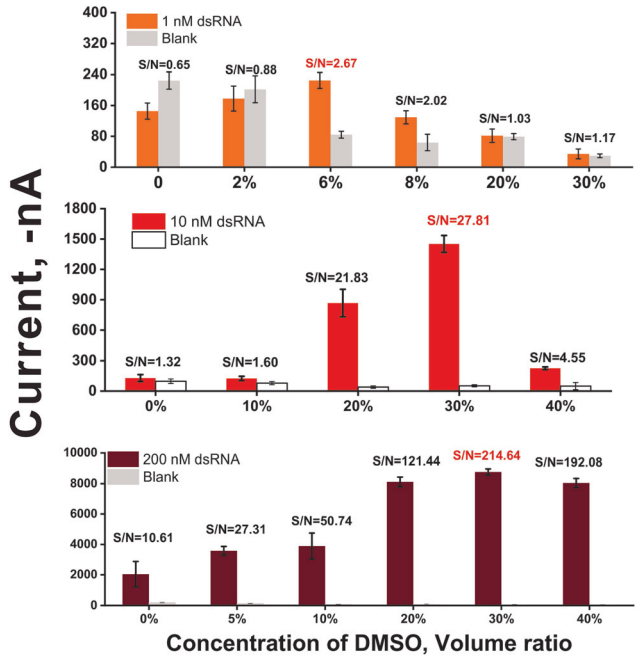

Fig. 2 The analysis results of E-biosensors with different concentrations of DMSO using different concentrations of the target: (A) 1 nM, (B) 10 nM, and (C) 200 nM. (The error bars were based on three repetitive experiments.)

systems were compared. Firstly, we applied only one reporter probe adjacent to the capture probe (Fig. 3Aa), and just as anticipated, the current signal was quite low due to the incomplete unfolding of the long RNA and the smaller amount of the combined biotin-labeled probes (Fig. 3B). In the second strategy (Fig. 3Ab), all the reporter probes (12 RPs and 2 spacers) were combined onto one side of the stem-loop RNA, while the third strategy distributed the reporter probes on two sides of the RNA (Fig. 3Ac). Finally, the third strategy achieved the highest S/N ratio, which we believe is mainly attributed to the decreased steric hindrance for the hybridization (Fig. 3B), on the other side, the free reporter probes in a and b produced much higher unspecific absorption and increased the current background.

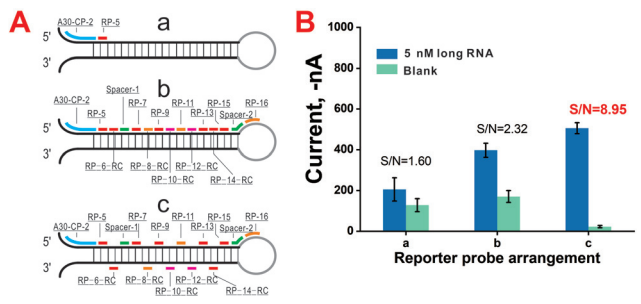

Fig. 3 The electrochemical measurement results of different reporter probes: (A) 3 different groups of reporter probes hybridized at different positions on the target long RNA molecule, (B) analysis results of 5 nM long RNA using different groups of reporter probes. (The error bars were based on three repetitive experiments.)

Structural analysis on the electrochemical interface

For the development of RNAi GMO technology, it is very important not only to sense the transcription of the long RNA, but also to understand the conformational change of the RNA from a stem-loop strand to a long dsRNA and finally to many functional siRNAs in the body of insects. One irreplaceable advantage of our MRP system was the potential addressable structural analysis. By using multi-channel electrochemical chips, we can perform parallel testing with different reporter probes at designed hybridization positions.

Three electrodes were prepared with the same polyA capture probe, but 3 different reporter probes, RP-5, RP-16 and RP-5-RC, were later added for the analysis of the target RNA (Fig. 4A). Three reporter probes were designed to hybridize at the 5′ end, the loop section and the 3′ end of the long stem-loop RNA, respectively. By using the 3-electrode parallel testing, we successfully performed the recognition of different structures of the RNA: (1) the intact long stem-loop RNA was capable of combing all 3 reporter probes, thus 3 electrochemical biosensors produced 3 positive current signals (top Fig. 4B). (2) The dsRNA without a loop section was analyzed (middle Fig. 4B). Since the dsRNA melting step of the biosensor, the complementary RNA was washed away and thus only RP-5 remains on the electrode surface. As shown in the middle of Fig. 4, only RP-5 showed a positive signal. (3) Short siRNAs were produced from the treatment of long RNA by RNaseIII (Fig. S2†), and negative signals were achieved by using all 3 different reporter probes (bottom Fig. 4B) since they were too short for either capture or reporter probes.

The sensitivity of the polyA-based E-biosensor

The optimized E-biosensor was used to detect a series of RNA solutions (Long stem-loop RNA, 1 pM–300 nM). The I–t method was performed for 60 s to achieve a steady current signal. As shown in Fig. 5, the current signal increased with the concentration of the long RNA, until it reached a plateau at about 200 nM. A nonlinear fitting relationship was demonstrated between the current and the RNA concentration: $y = -4770\ \exp(-x/48\,214) + 4813$, where y is the current and x is the concentration of RNA. The limit of detection (LOD) was proved to be 1 pM.

Analysis of total RNA from RNAi-based transgenic maize leaf tissue

The practicability of our biosensor was challenged by detecting total RNA from RNAi-based transgenic maize leaves. 4 different RNA samples were extracted and analyzed: 11061-P was the specific target, 11048-P and 11019-P were two similar stem-loop long RNA molecules with different "stem" sequences (Fig. 5B), and 11061-N was from a non-transgenic maize leaf tissue. As shown in Fig. 5, the current signals for non-complementary and non-transgenic RNAi were as low as blank, and the current signal for the target RNA was about 192

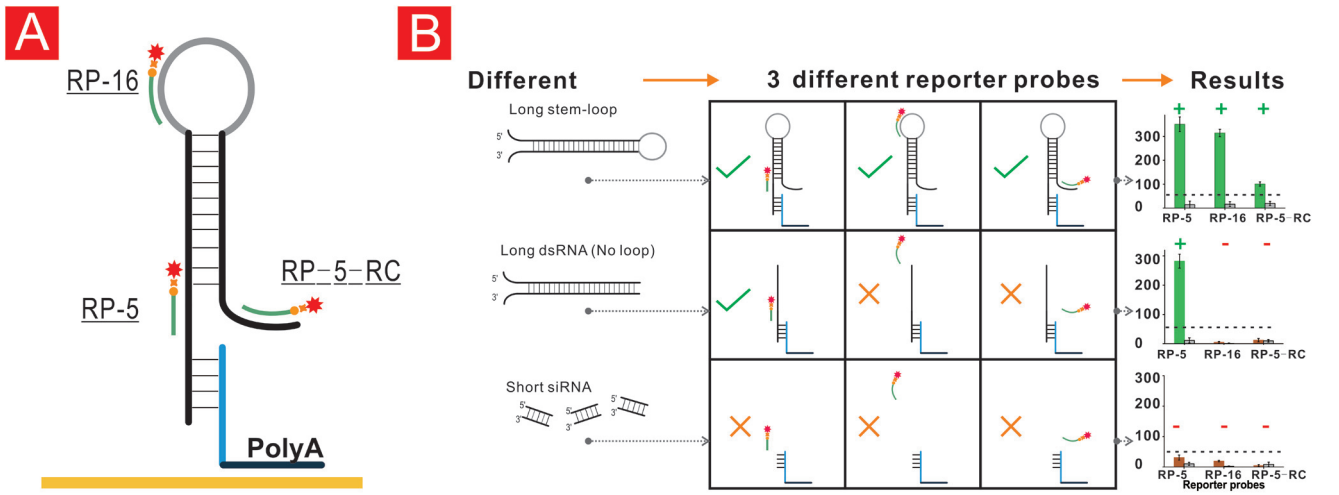

Fig. 4 (A) The strategy of structural analysis by simultaneously using 3 different reporter probes, (B) the corresponding analysis results of each structure of the RNA molecule: long stem-loop RNA, long dsRNA (no loop) and short siRNA. (The error bars were based on three repetitive experiments.)

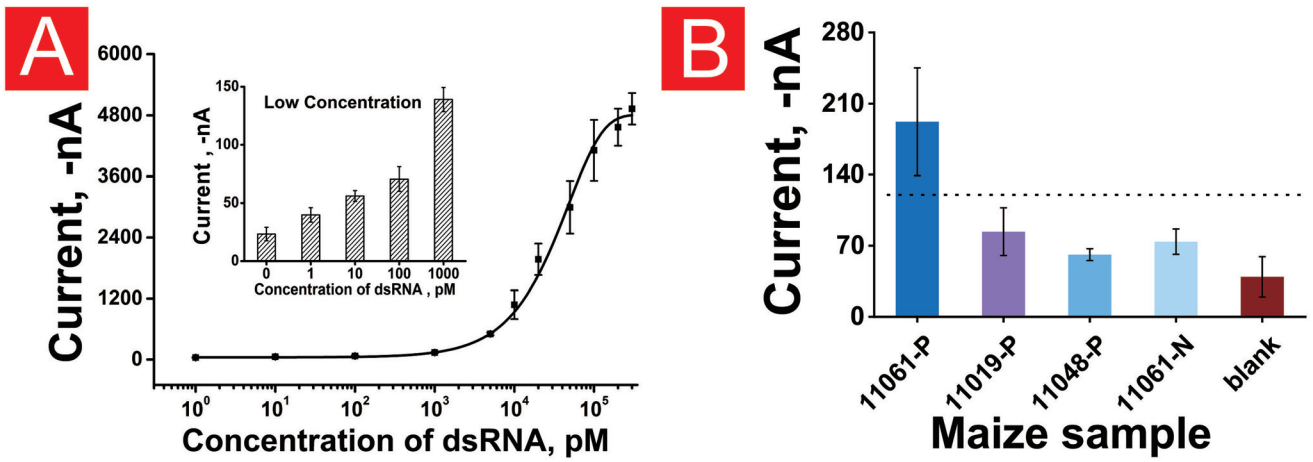

Fig. 5 A) The working curve of our E-biosensor. The inserted histogram showed the results of low concentration of RNA and a buffer solution as the blank. The target was an in vitro transcribed RNA (1034 nt, Section 2.2). B) Analysis of total RNA from 4 RNAi-based transgenic maize leaves: the target 11061-P, three negative control (11019-P, 11048-P and 11061-N) and a buffer solution as the blank. Error bars are the SD of three repetitive experiments.

nA. By using the working curve in Fig. 5A, the concentration of the long RNA was calculated to be 0.5 ng μL^{-1}, which was 1/7275 of the total RNA (3637.5 ng μL^{-1}). The signal of the specific target was proved to be about 3 times higher than the non-specific target and the blank, demonstrating the selectivity of our biosensor even facing real plant samples. The concentration of 4 total RNA samples extracted from RNAi-based transgenic maize leaves was validated using a digital PCR (dPCR), which is widely recognized as an absolute quantification method for nucleic acid (Table S1†).

Signal amplification using RT-RPA

To further improve the sensitivity and detection limit, RT-RPA was performed to produce a 379 bp double-strand DNA

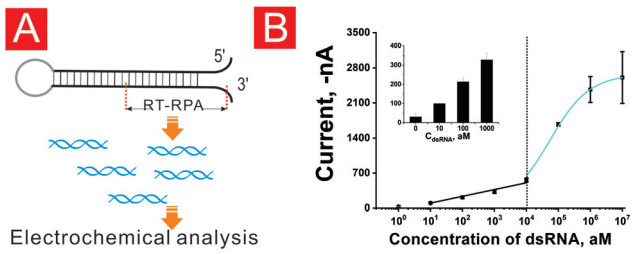

Fig. 6 (A) The reaction of RT-RPA followed by E-biosensors, (B) Analysis result of the RT-RPA amplification product of the long RNA. (The insert column plots showed the results of low concentration and the blank, and the error bars were based on three repetitive experiments.)

(dsDNA) from the target RNA. As indicated in Fig. 6, after RT-RPA amplification, the detection sensitivity was enhanced. For high concentration (10 fM–10 pM), the current signal increased with the concentration with a nonlinear fitting relationship. For low concentration (10 aM–10 fM), an excellent positive linear relationship was constructed between the current and the RNA concentration. Finally, 10 aM RNA was successfully detected.

Conclusions

For RNAi GMO in agricultural biotechnology, the efficient transcription of the RNA molecule is a critical premise. Thus, the amount of designed RNA was recognized as a specific indicator, for both safety and functional assessment of RNAi GMO. Facing the challenge of the length and the complex secondary structure for the analysis of long RNA, we developed a novel electrochemical biosensor, based on a polyA DNA probe. 3 main signs of progress were achieved: (1) the optimized polyA self-assembling monolayer (SAM) showed advanced surface density and stability on the interface, which is critical for the subsequent hybridization of very large RNA molecules. (2) For the detection of the long RNA, we developed a multi-reporter probe system. 12 RPs combined onto the RNA at different positions. Interestingly, DMSO was found to be capable of improving the unfolding efficiency of the RNA secondary structure and promoting the competitive hybridization of the probes. (3) The detection practicability was demonstrated during the analysis of 1 pM–300 nM long target RNA, and good selectivity was achieved when directly analyzing extracted total RNA from transgenic maize lines. More impressively, when RT-RPA technology was combined with our biosensor, the sensitivity was further improved to as low as 10 aM. In summary, the E-biosensor showed advanced analysis capability for RNAi GMO products and provided great potential for the field test of long RNA in a wide range of biological samples.

Author contributions

Li Xu and Jiawei Qi performed the electrochemical analysis. Yanli Wen, Wen Liang, and Lele Wang finished the data analysis. Liang Li, Zhenzhou Yang, Xue Yang, Yu Qi, and Manlei Duan prepared the plant sample. Li Xu, Keke Zhao, Jie Gu, and Yiji Shen finished the RNA *in vitro* transcription. Liang Li and Pinhua Rao did the review and editing of the draft. Gang Liu wrote the manuscript and was in charge of the submission.

Conflicts of interest

There are no conflicts to declare.

Acknowledgements

This work was financially supported by the National Quality Infrastructure Program of China (2018YFF0212800), the Technical standards Project of the Science and Technology Innovation Action Plan (18DZ2201700), the National Major Special Project for the Development of Transgenic Organisms (2018ZX08011-04B), the National Natural Science Foundation of China (No. 21775104, 22074093, and 11705270), and the Youth Innovation Promotion Association of CAS (2012205). We would like to thank Beijing Dabeinong Biotechnology Co., Ltd. for kindly providing the transgenic maize.

References

1 A. Fire, S. Xu, M. K. Montgomery, S. A. Kostas, S. E. Driver and C. C. Mello, *Nature*, 1998, **391**, 806–811.
2 G. J. Hannon, *Nature*, 2002, **418**, 244–251.
3 A. Dalakouras, M. Wassenegger, E. Dadami, I. Ganopoulos, M. L. Pappas and K. Papadopoulou, *Plant Physiol.*, 2020, **182**, 38–50.
4 J. A. Baum, T. Bogaert, W. Clinton, G. R. Heck, P. Feldmann, O. Ilagan, S. Johnson, G. Plaetinck, T. Munyikwa, M. Pleau, T. Vaughn and J. Roberts, *Nat. Biotechnol.*, 2007, **25**, 1322–1326.
5 F. Liu, B. Yang, A. Zhang, D. Ding and G. Wang, *Front. Plant Sci.*, 2019, **10**, 64.
6 X. D. Yu, Z. C. Liu, S. L. Huang, Z. Q. Chen, Y. W. Sun, P. F. Duan, Y. Z. Ma and L. Q. Xia, *Pest Manage. Sci.*, 2016, **72**, 1090–1098.
7 S. J. Cronin, N. T. Nehme, S. Limmer, S. Liegeois, J. A. Pospisilik, D. Schramek, A. Leibbrandt, M. Simoes R de, S. Gruber, U. Puc, I. Ebersberger, T. Zoranovic, G. G. Neely, A. von Haeseler, D. Ferrandon and J. M. Penninger, *Science*, 2009, **325**, 340–343.
8 D. Nowara, A. Gay, C. Lacomme, J. Shaw, C. Ridout, D. Douchkov, G. Hensel, J. Kumlehn and P. Schweizer, *Plant Cell*, 2010, **22**, 3130–3141.
9 V. Bitko, A. Musiyenko, O. Shulyayeva and S. Barik, *Nat. Med.*, 2005, **11**, 50–55.
10 D. Palliser, D. Chowdhury, Q. Y. Wang, S. J. Lee, R. T. Bronson, D. M. Knipe and J. Lieberman, *Nature*, 2006, **439**, 89–94.
11 A. Alakonya, R. Kumar, D. Koenig, S. Kimura, B. Townsley, S. Runo, H. M. Garces, J. Kang, A. Yanez, R. David-Schwartz, J. Machuka and N. Sinha, *Plant Cell*, 2012, **24**, 3153–3166.
12 B. Mamta and M. V. Rajam, *Physiol. Mol. Biol. Plants*, 2017, **23**, 487–501.
13 J. A. Heinemann, S. Z. Agapito-Tenfen and J. A. Carman, *Environ. Int.*, 2013, **55**, 43–55.
14 S. Arpaia, A. N. E. Birch, J. Kiss, J. J. A. van Loon, A. Messean, M. Nuti, J. N. Perry, J. B. Sweet and C. C. Tebbe, *Sci. Total Environ.*, 2017, **583**, 123–132.

15 J. M. Casacuberta, Y. Devos, P. du Jardin, M. Ramon, H. Vaucheret and F. Nogue, *Trends Biotechnol.*, 2015, **33**, 145–147.
16 W. Parrott, B. Chassy, J. Ligon, L. Meyer, J. Petrick, J. Zhou, R. Herman, B. Delaney and M. Levine, *Food Chem. Toxicol.*, 2010, **48**, 1773–1790.
17 S. A. Bustin, *J. Mol. Endocrinol.*, 2000, **25**, 169–193.
18 T. A. Armstrong, H. Chen, T. E. Ziegler, K. R. Iyadurai, A. G. Gao, Y. Wang, Z. Song, Q. Tian, Q. Zhang, J. M. Ward, G. C. Segers, G. R. Heck and J. M. Staub, *J. Agric. Food Chem.*, 2013, **61**, 12557–12564.
19 M. Lin, Y. Wen, L. Li, H. Pei, G. Liu, H. Song, X. Zuo, C. Fan and Q. Huang, *Anal. Chem.*, 2014, **86**, 2285–2288.
20 J. Wang, *Biosens. Bioelectron.*, 2006, **21**, 1887–1892.
21 D. W. Kimmel, G. LeBlanc, M. E. Meschievitz and D. E. Cliffel, *Anal. Chem.*, 2012, **84**, 685–707.
22 Y. Wen, H. Pei, Y. Shen, J. Xi, M. Lin, N. Lu, X. Shen, J. Li and C. Fan, *Sci. Rep.*, 2012, **2**, 867.
23 Z. Li, C. Wang, J. Li, J. Zhang, C. Fan, I. Willner and H. Tian, *CCS Chem.*, 2020, **2**, 707–728.
24 Y. Lee, J. Choi, H. K. Han, S. Park, S. Y. Park, C. Park, C. Baek, T. Lee and J. Min, *Sens. Actuators, B*, 2021, **326**, 7.
25 Y. H. Cheng, S. J. Liu and J. H. Jiang, *Talanta*, 2021, **222**, 8.
26 Y. Sheng, T. H. Zhang, S. H. Zhang, M. Johnston, X. H. Zheng, Y. Y. Shan, T. Liu, Z. N. Huang, F. Y. Qian, Z. H. Xie, Y. R. Ai, H. K. Zhong, T. R. Kuang, C. Dincer, G. A. Urban and J. M. Hu, *Biosens. Bioelectron.*, 2021, **178**, 10.
27 J. Zhang, S. Song, L. Wang, D. Pan and C. Fan, *Nat. Protoc.*, 2007, **2**, 2888–2895.
28 L. Xu, W. Liang, Y. Wen, L. Wang, X. Yang, S. Ren, N. Jia, X. Zuo and G. Liu, *Biosens. Bioelectron.*, 2018, **99**, 424–430.
29 X. Wang, H. J. Lim and A. Son, *Environ Health Toxicol*, 2014, **29**, e2014007.
30 C. R. Flores-Juarez, E. Gonzalez-Jasso, A. Antaramian and R. C. Pless, *BioTechniques*, 2016, **61**, 175–182.
31 M. R. Green and J. Sambrook, *Cold Spring Harb. Protoc.*, 2019, **2019**(2), DOI: 10.1101/pdb.prot095141, PMID: 30710022.
32 C. Song, E. Castellanos-Rizaldos, R. Bejar, B. L. Ebert and G. M. Makrigiorgos, *Clin. Chem.*, 2015, **61**, 1354–1362.
33 N. Chester and D. R. Marshak, *Anal. Biochem.*, 1993, **209**, 284–290.